

Cell Biology

# Adhesion of freshwater sponge cells mediated by carbohydrate–carbohydrate interactions requires low environmental calcium

Eduardo Vilanova<sup>2</sup>, Priscilla J Ciodaro<sup>2</sup>, Francisco F Bezerra<sup>2</sup>, Gustavo RC Santos<sup>2</sup>, Juan J Valle-Delgado<sup>3</sup>, Dario Anselmetti<sup>4</sup>, Xavier Fernàndez-Busquets<sup>5,6,1</sup> and Paulo AS Mourão<sup>2,1</sup>

<sup>2</sup>Instituto de Bioquímica Médica Leopoldo de Meis and Hospital Universitário Clementino Fraga Filho, Universidade Federal do Rio de Janeiro, Rio de Janeiro 21941-913, Brazil, <sup>3</sup>Department of Bioproducts and Biosystems, School of Chemical Engineering, Aalto University, Aalto FI-00076, Finland, <sup>4</sup>Experimental Biophysics and Applied Nanoscience, Faculty of Physics, Bielefeld University, Bielefeld 33615, Germany, <sup>5</sup>Barcelona Institute for Global Health (ISGlobal), Hospital Clínic-Universitat de Barcelona, Barcelona ES-08036, Spain, and <sup>6</sup>Nanomalaria Group, Institute for Bioengineering of Catalonia (IBEC), The Barcelona Institute of Science and Technology, Barcelona ES-08028, Spain

<sup>1</sup>To whom correspondence should be addressed: Tel/Fax: +34-93-227-5400, e-mail: xfernandez\_busquets@ub.edu (Xavier Fernàndez-Busquets); Tel/Fax: +55-21-3938-2090, pmourao@hucff.ufrj.br (Paulo AS Mourão)

Received 6 August 2019; Revised 11 February 2020; Editorial Decision 11 February 2020; Accepted 13 February 2020

## Abstract

Marine ancestors of freshwater sponges had to undergo a series of physiological adaptations to colonize harsh and heterogeneous limnic environments. Besides reduced salinity, river-lake systems also have calcium concentrations far lower than seawater. Cell adhesion in sponges is mediated by calcium-dependent multivalent self-interactions of sulfated polysaccharide components of membrane-bound proteoglycans named aggregation factors. Cells of marine sponges require seawater average calcium concentration (10 mM) to sustain adhesion promoted by aggregation factors. We demonstrate here that the freshwater sponge *Spongilla alba* can thrive in a calcium-poor aquatic environment and that their cells are able to aggregate and form primmorphs with calcium concentrations 40-fold lower than that required by marine sponges cells. We also find that their gemmules need calcium and other micronutrients to hatch and generate new sponges. The sulfated polysaccharide purified from *S. alba* has sulfate content and molecular size notably lower than those from marine sponges. Nuclear magnetic resonance analyses indicated that it is composed of a central backbone of non- and 2-sulfated  $\alpha$ - and  $\beta$ -glucose units decorated with branches of  $\alpha$ -glucose. Assessments with atomic force microscopy/single-molecule force spectroscopy show that *S. alba* glucan requires 10-fold less calcium than sulfated polysaccharides from marine sponges to self-interact efficiently. Such an ability to retain multicellular morphology with low environmental calcium must have been a crucial evolutionary step for freshwater sponges to successfully colonize inland waters.

**Key words:** carbohydrate interactions, evolutionary adaptation, Porifera, proteoglycans, sulfated polysaccharides

## Introduction

Sponges (phylum Porifera) likely emerged in Precambrian 800 Ma (mega-annum), which makes these sessile filter-feeding animals the oldest extant metazoans (Fernández-Busquets 2010). Although marine sponge body fossils are found in shales dated between 660 and 635 Ma (Cryogenian period), most of freshwater sponges fossil records (>99.5%) are much more recent, dating back up to the Miocene epoch (~23 Ma) (Maloof et al. 2010; Pronzato et al. 2017). The remarkable gap between emergence of marine and freshwater sponges possibly relates to the extensive set of evolutionary adaptations that were necessary for such simple marine animals, in which the metabolism operates basically at cellular level, to succeed in colonizing freshwater habitats such as lakes and rivers (e.g. osmotic regulation and micronutrients requirement) (Erpenbeck et al. 2011). Besides physiological adaptations, most freshwater sponges have also developed gemmules, which are specialized resting bodies crucial to their viability in harsh limnic environments (Manconi and Pronzato 2008).

Gemmules are resistant asexual reproductive bodies composed of modified archeocytes named thesocytes, in which the cytoplasm is full of reserve material stored into vitelline compartments, which are enveloped by a noncellular outer layer constructed by specialized spicules (gemmulescleres) (Funayama 2013). When the environmental conditions are favorable for the sponge to thrive, gemmules stay dormant inside their bodies; however, in the advent of drought or winter freeze, sponge tissues are degraded but gemmules can endure desiccation and freezing for long periods in a cryptobiotic state (Manconi and Pronzato 2016). As soon the environmental conditions become propitious again, the gemmules hatch and then their thesocytes undergo mitosis, becoming either histoblasts or totipotent archeocytes, which migrate outwards, proliferate and differentiate into all the cell-types necessary to generate a fully functional sponge (Bart et al. 2019). Besides gemmules, freshwater sponges also produce primmorphs, which are less resistant resting bodies built of nonmodified archeocytes surrounded by an epithelial outer layer reinforced with spongin (e.g. Vilanova et al. 2010; Annenkov and Danilovtseva 2016).

In most animals, cell–cell adhesion is promoted by proteins, such as cadherins, occludins and connexins (Abedin and King 2010); however, intercellular adhesion and recognition in sponges are mediated by proteoglycan-like molecules named aggregation factors (AFs) (Jarchow et al. 2000). The supramolecular structure of AFs resembles that of mammalian aggrecans: large, extracellular membrane bound, aggregating and modular proteoglycans (Fernández-Busquets and Burger 2003). The AF of the marine sponge *Clathria prolifera* (Figure 1A) is composed of a circular protein core attached to two different carbohydrate units: a small 6-kDa glycan that mediates the interaction of the AF with putative receptors present in the cell membrane and a larger 200-kDa sulfated polysaccharide (SP), which binds homophilically with identical units on the AFs of adjacent cells (Blumbach et al. 1998; Garcia-Manyes et al. 2006).

AF SPs use to have very complex chemical structures, being often composed of an intricate set of different sugars (e.g. glucose, fucose and arabinose), with a variety of sulfation patterns, as well as of other acidic sugars, such as hexuronic acid and pyruvated galactose (Vilanova et al. 2008). A good example is the SP from the marine sponge *Desmapsamma anchorata*; the comprehensive set of nuclear magnetic resonance (NMR) analyses employed to investigate its structure revealed the presence of a central backbone composed of [1 → 3]-linked nonsulfated and 2,4-disulfated  $\alpha$ -glucose,

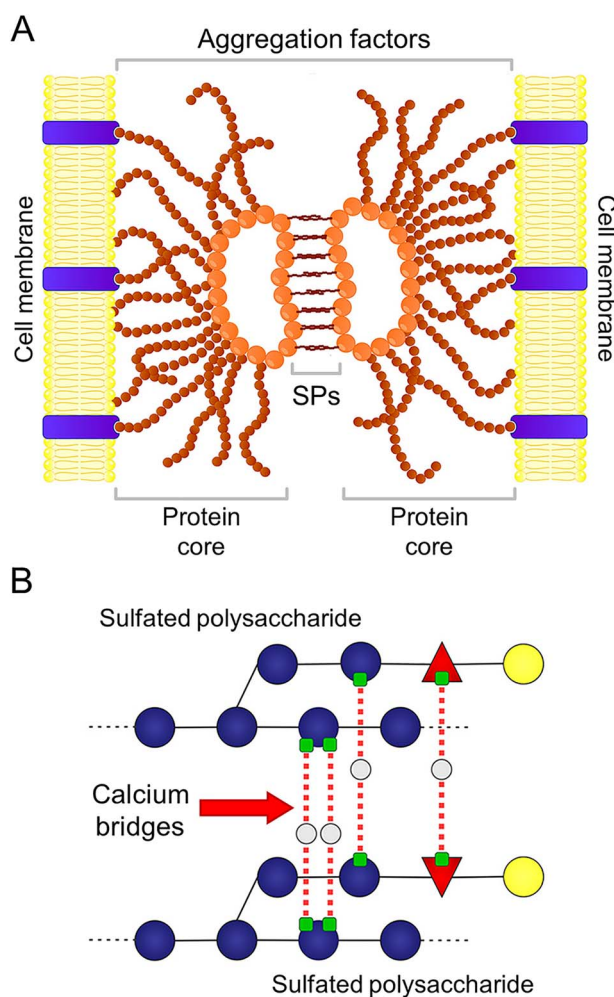


**Fig. 1.** Structural features of aggregation factors and self-interactions mediated by “calcium bridges”. (A) The aggregation factor (AF) of the marine sponge *Clathria prolifera* is built of a “ring” of globular protein units (in orange) linked either to sulfated polysaccharides (SPs) responsible for the cell–cell adhesion or protein “arms” (in brown) involved in the binding with cell membrane receptors (in blue). (B) Self-interactions of SP components of *Desmapsamma anchorata* AF are promoted by “calcium bridges” (red pointed-lines) between sulfate groups (green squares) on their glucose (blue circles) and fucose (red triangles) units mediated by extracellular calcium (gray circles). Both panels are modified from Vilanova et al. (2016). This figure is available in black and white in print and in colour at *Glycobiology* online.

which is decorated with branches of 4,6-pyruvated  $\alpha$ -galactose [1 → 3] 2-sulfated  $\alpha$ -fucose [1 → 3] 4-sulfated  $\alpha$ -glucose [1 → 3]  $\alpha$ -glucose [1 → 4]-linked to nonsulfated  $\alpha$ -glucose units of the backbone (Vilanova et al. 2016). Besides intrinsic complexity, SPs from marine sponges also present species-specific chemical compositions (Vilanova et al. 2008, 2016).

Previous reports based on cellular and noncellular assays have shown that the multivalent self-interactions of AF SPs that sustain sponge cell adhesion are calcium-dependent and species-specific (e.g. Bucior et al. 2004; Misevic et al. 2004; Vilanova et al. 2009). Assessments with atomic force microscopy/single-molecule force spectroscopy (AFM/SMFS) demonstrated that the homophilic interactions of *D. anchorata* SPs (Figure 1B) are mediated by “calcium bridges” between their sulfate groups (Vilanova et al.

2016). Moreover, simulations based on dynamic force spectroscopy (AFM/DFS) data from self-interactions of *C. prolifera* SP indicate that sponge cell mean disaggregation time is far shorter in calcium-deficient (0 mM) than in calcium-rich (10 mM) environments (Fernández-Busquets et al. 2009).

Seawater chemical composition is remarkably homogenous; except for minor variations in estuary and coral areas, calcium concentration in seawater is about 400 mg/L (~10 mM) (Millero et al. 2008). On the other hand, chemical composition of inland waters may vary at extreme levels. River-lake systems often contain calcium concentrations far lower (1–2 mg/L) than seawater; however, some freshwater bodies in limestone areas have up to 100 mg/L calcium (Potasznik and Szymczyk 2015). In the present study, we show that the freshwater sponge *Spongilla alba* thrives in a calcium-poor aquatic environment and that their cells are able to aggregate and produce primmorphs with calcium concentrations far lower than that required by cells of marine sponges; moreover, we find that their gemmules demand calcium and other micronutrients to hatch and generate new sponges. The SP with reduced sulfate content and molecular size purified from *S. alba* had its unique structure investigated with solution NMR. We also demonstrate with AFM/SMFS assays that the branched glucan from *S. alba* self-interact efficiently with low calcium concentrations. Considering that subtle variations seem to be determinant for viability of different species, environmental calcium might be an important parameter to increase the understanding on biogeographical distribution of freshwater sponges.

## Results

### *Spongilla alba* is able to thrive in a calcium-poor freshwater environment

Considering that the freshwater sponge *S. alba* (Supplementary Figure S1), which was employed as a model in our study, was collected in a costal lake that is separated from the sea by a narrow sand bank (Supplementary Figure S1), we analyzed the lake's water to evaluate whether that proximity to seawater could influence its chemical composition. Seawater has an average salinity of 35 ppt (mg/ton), whereas the salinity of Lake Carapebus was trace when expressed as ppt (Supplementary Table SI), and thus, it is a genuine freshwater lake. Such a reduced salinity was due to low concentrations of major constituents of seawater, including chloride, sulfate, sodium, magnesium, calcium and potassium (Supplementary Table SI). The calcium concentration of Lake Carapebus water (~7 mg/L) is approximately 50-fold lower than that of seawater (~400 mg/L) and, therefore, *S. alba* is able to thrive in a calcium-poor freshwater environment. Chemical parameters presented in Supplementary Table SI were used as a basis to prepare the media (CMFFW and M-medium) employed in our in vitro and AFM/SMFS assays.

### *S. alba* cells aggregate with low calcium concentrations

Once the water chemistry of *S. alba*'s habitat was determined, we were able to prepare media (CMFFW) suitable to evaluate the calcium concentration required to promote in vitro cell aggregation. As expected, *S. alba* cells kept in CMFFW supplemented with EDTA did not aggregate (Figure 2A); otherwise, cells incubated in CMFFW containing different concentrations of calcium yielded aggregates with distinct features. Cells subjected to 0.1 mM CaCl<sub>2</sub> formed friable aggregates significantly smaller and more abundant ( $P < 0.05$ ) than

those formed at higher CaCl<sub>2</sub> concentrations (Figure 2B–F). Despite the noticeable but nonsignificant ( $P > 0.05$ ) difference observed in their sizes (Figure 2F), aggregates formed either at 0.25 or 0.5 mM CaCl<sub>2</sub> were quite resilient, being able to resist mechanical stress promoted by vigorous agitation of the incubation media. We also find that the minimum calcium concentration (0.25 mM CaCl<sub>2</sub>) that was necessary to form consistent aggregates in our assays is in strict accordance with the calcium concentration (~0.2 mM) of Lake Carapebus water.

### *S. alba* cells form primmorphs with low calcium concentrations

After ascertaining the calcium requirements to promote cell aggregation, we assessed the capability of *S. alba* cells kept in culture with different calcium concentrations to produce primmorphs. Aggregates formed in CMFFW supplemented with 0.1 mM CaCl<sub>2</sub> disintegrated when detached from the substrate and thus were unable to generate primmorphs. On the other hand, cultures performed either with 0.25 or 0.5 mM CaCl<sub>2</sub> yielded primmorphs. On the first day, dissociated cells (Figure 3A) incubated in CMFFW containing 0.25 mM CaCl<sub>2</sub> bound actively, forming small and irregular aggregates (Figure 3B). During the second and third days, the aggregates grew irregularly by connecting one to each other (Figure 3C and D). On the fourth and fifth days, the aggregates ceased to interconnect, increased in size and acquired the round shape and smooth surface characteristic of mature primmorphs (Figure 3E and F). Cultures conducted with 0.5 mM CaCl<sub>2</sub> produced primmorphs in a similar manner (data not shown).

Our histological analyses showed that *S. alba* primmorphs are constituted by an inner mass of archeocytes and lophocytes surrounded by an outer layer built of pinacocytes (Figure 3G). Totipotent archeocytes were significantly more abundant ( $P < 0.001$ ) than spongin-secreting lophocytes and peripheral pinacocytes (Figure 3H). In addition, staining of the sections with toluidine blue revealed an intense metachromasy (purple stain) in the primmorph cells, especially in archeocytes, which indicates the presence of intracellular and/or pericellular SPs (Figure 3G). These results demonstrate that primary cultures of *S. alba* cells performed with media containing reduced calcium concentrations (up to ~0.2 mM) can generate typical primmorphs

### *S. alba* gemmules require calcium to hatch

Considering that freshwater sponges depend on their gemmules to endure seasonal drought and freeze of rivers and lakes, we investigated with in vitro assays whether calcium participates in their hatching and development as new sponges. *S. alba* gemmules incubated for up to 30 days in M-medium containing either EDTA or different concentrations of CaCl<sub>2</sub> (0.1 → 0.5 mM), which encompasses the calcium concentration of Lake Carapebus water (~0.2 mM), did not hatch. On the other hand, 60% of the gemmules (9 out of 15) kept in natural water from Lake Carapebus (LCW) hatched after 8 days (Figure 4A). Accordingly, we proceeded with the evaluation of the role of calcium in the hatching of these gemmules by incubating them in LCW supplemented with EDTA or EGTA. As seen in the assays conducted with M-medium, gemmules kept in LCW containing either unspecific (EDTA) or specific (EGTA) calcium-chelators did not hatch after 30 days incubation. These results indicate that hatching of *S. alba* gemmules requires calcium, as well as other micronutrients present in LCW and not in our modified M-medium.



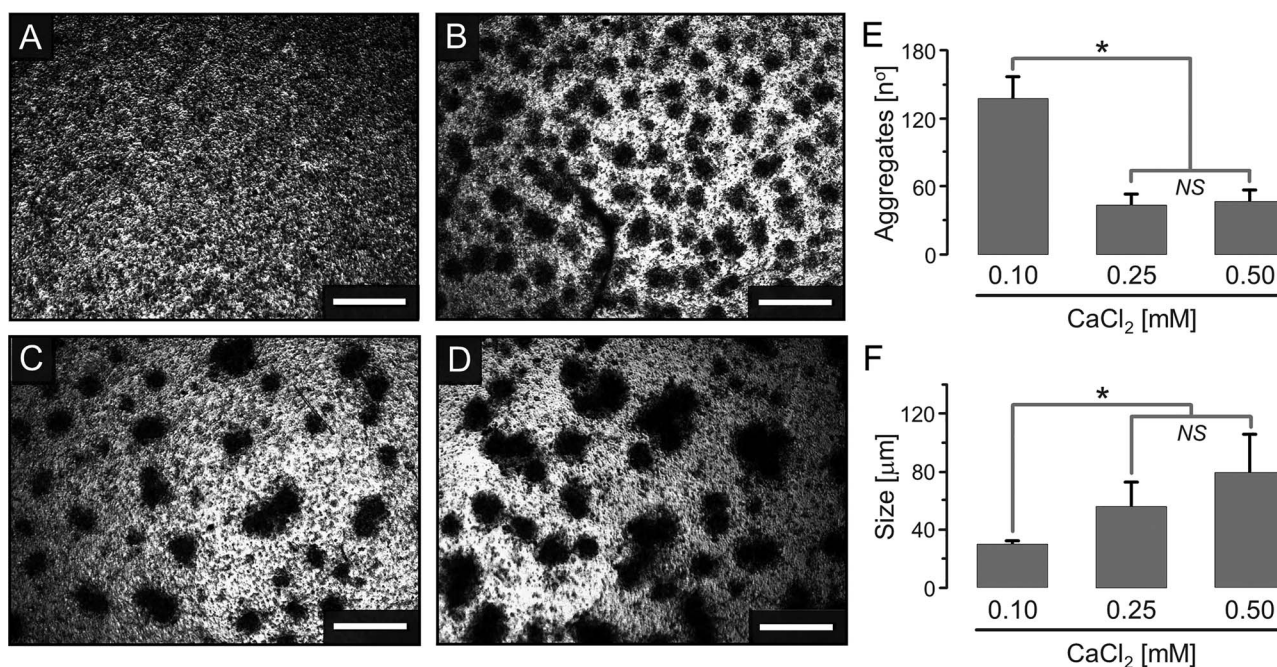


**Figure 2.** Aggregation of *Spongilla alba* cells with different calcium concentrations. Dissociated cells were incubated for 1 h in CMFFW supplemented with 2.5 mM EDTA (A) or 0.10 (B), 0.25 (C) and 0.50 (D) mM  $\text{CaCl}_2$ ; scale bars = 100  $\mu\text{M}$ . Number (E) and size (F) of the aggregates (mean  $\pm$  S.D.) formed by cells incubated at different calcium concentrations (triplicates, 10 random fields per plate) were compared by ANOVA; \* $P < 0.05$  and NS  $P > 0.05$ . This figure is available in black and white in print and in colour at *Glycobiology* online.

Then, we followed the initial development of the sponges generated by *S. alba* gemmules. On the first 2 days after hatching (Figure 4A), archeocytes and histiocytes migrated outwards and proliferated actively on the substrate around the gemmules (Figure 4B). Over the next 4 days (Figure 4C and D), histiocytes became basopinacocytes and archeocytes differentiated into a variety of cell types (e.g. choanocytes and sclerocytes), which began the formation of the basal pinacoderm (Figure 4E), aquiferous system (Figure 4F and G) and siliceous skeleton (spiculogenesis) (Figure 4H and I). Thereafter, the choanosome and skeleton underwent further organization and an ectosome lining the outer surface (Figure 4J) and an osculum (Figure 4K) formed, giving origin to fully functional miniature sponges 6 days after the hatching. We also observed that the sponges in formation released a great number of motile archeocytes toward the adjacent substrate (Figure 4L), which in turn must act as phagocytes in the defense against pathogens and foreign body invasion (Johnston and Hildemann 1982).

#### The sulfated polysaccharide from *S. alba* has reduced sulfate content and molecular size

After assessing cell interactions with in vitro assays, we proceeded with purification and chemical analysis of the SP from *S. alba* to investigate in further detail the calcium-dependent self-interactions responsible for sustaining cell adhesion. Crude polysaccharide extracts from *S. alba* were applied into a Q-Sepharose column and then eluted through a linear NaCl gradient, yielding chromatograms with two peaks, which were collected as distinct fractions identified as G8 and G20 (Figure 5A). Agarose gel electrophoresis of G8 revealed a polydisperse polysaccharide with low metachromasy whereas G20 is homogeneous and fairly stained by toluidin blue (Figure 5B). Molecular size estimations with polyacrylamide gel

electrophoresis confirmed that G20 has a mass of approximately 20 kDa and a homogenous molecular weight distribution; on the other hand, G8 presented a highly polydisperse distribution and molecular weight around 8 kDa (Figure 5C). Chemical analyses revealed that both fractions do not contain carboxylated and pyruvated sugars and that G20 is more sulfated than G8 (Supplementary Table SII). Its high polydispersity, small size and low sulfate content suggest that G8 is degraded G20 rather than an intact and functional SP expressed in the cells of the sponge; for this reason, we designated G20 as the putative SP component of *S. alba* AF.

Analyses with gas-chromatography/mass spectroscopy (GC/MS) demonstrated that G20 is composed exclusively of glucose (Supplementary Figure S2). Despite the small quantity of purified G20 (~2 mg), we investigated its chemical structure with solution NMR techniques.  $^1\text{H}/^{13}\text{C}$  HSQC spectrum of G20 revealed the presence of five well-resolved signals resonating in the region of anomeric protons/carbons (H1/C1) of  $\alpha$ - (units A  $\rightarrow$  D) and  $\beta$ - (unit E) glucose anomers (Figure 6A).  $^1\text{H}/^{13}\text{C}$  chemical shifts and the proportions of the units A  $\rightarrow$  E are reported in Table I. Along with anomeric signals, we have also identified on the 1D  $^1\text{H}$  spectrum of G20 (Supplementary Figure S3) a well resolved signal resonating at high-field (1.28 ppm), which is characteristic of  $\text{CH}_3$  groups of methyl sugars (Vilanova et al. 2016); however, our GC/MS analyses clearly show the absence of methyl sugars (e.g. fucose and rhamnose) in G20. That signal could also not be attributed to acetyl groups (~2.0 ppm) or pyruvate rings (~1.4–1.8 ppm), and thus, it possibly came from a non-carbohydrate contaminant (Vilanova et al. 2016).

Although we have identified anomeric signals on HSQC spectrum, the chemical structure of G20 cannot be fully characterized with solution NMR because of its high complexity and the scarce sample available to acquire the spectra, which eventually hinders

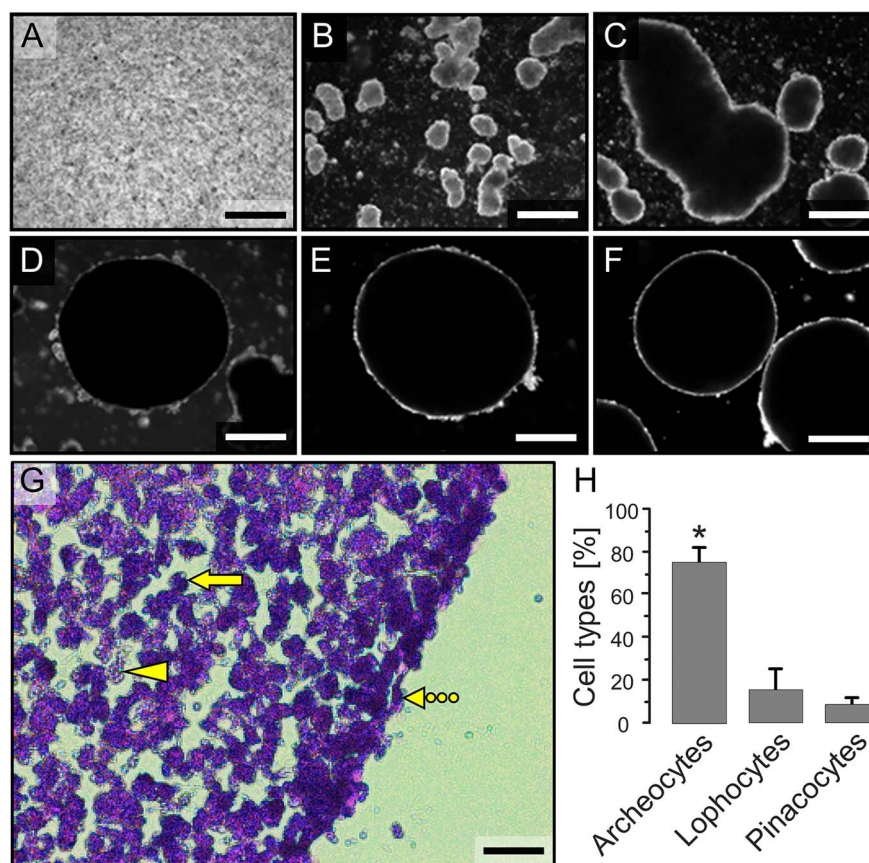


**Figure 3.** Primmorphs formed by *Spongilla alba* cells. Dissociated cells (A) incubated in CMFFW supplemented with 0.25 mM CaCl<sub>2</sub> aggregate actively during the first day (B). On the second (C) and third (D) days, the aggregates grown by connecting one to each other and on the fourth (E) and fifth (F) days they increase in size and acquire the round shape and smooth surface characteristic of primmorphs; scale bars = 500  $\mu$ m. (G) Primmorph section stained with toluidine blue; solid-arrow points out an archeocyte, arrowhead a lophocyte and dotted-arrow a pinacocyte, scale bar = 50  $\mu$ m. (H) Cell types (%) were quantified (mean  $\pm$  S.D.; 3 primmorphs) and compared by ANOVA; \* $P < 0.001$ . This figure is available in black and white in print and in colour at *Glycobiology* online.

detection or accurate assignment of some signals; notwithstanding, we were able to extract some information on G20 composition from further spectra. <sup>1</sup>H/<sup>1</sup>H TOCSY MLEV17 phase-sensitive (phase-TOCSY) spectrum of G20 (Figure 6B) differentiates protons coupled through scalar-coupling (phase-signals; Figure 6B, in blue) from those with dipolar-coupling (antiphase signals; Figure 6B, in red). Phase-TOCSY spectra have been increasingly employed to investigate structures of complex SPs, such as heparin, fucosylated chondroitin sulfate and the SP from *D. anchorata* (Vilanova et al. 2016; Tovar et al. 2016; Mourão et al. 2018). Assignment of in-phase cross-peaks on G20 phase-TOCSY spectrum allowed us to trace spin systems of the five units (A  $\rightarrow$  E) identified on the HSQC spectrum (Figure 6B, vertical black lines).

Position 2 of units B and D certainly is the sulfation site due to the characteristic  $\sim$ 0.6 ppm downfield shift of their H2 signals (Table I). It is not clear whether position 2 of the unit C also is sulfated because of its H2 signal is only 0.3 ppm downfield shifted (Table I). Positions 3 of unit B, 4 of unit D and 6 of unit E possibly are glycosylation sites due to typical downfield shifted of their carbon signals ( $\sim$ 4–6 ppm) (Table I). However, interpretation of these results is difficult because of the lack of further information on branched SPs composed of alternating  $\alpha$ - and  $\beta$ -glucose units with distinct sulfation patterns. Both the lack of reference chemical shifts and sample scarcity hindered precise identifications of glycoside bonds and, therefore, we investigated connections between the units only

with basis on correlations of anti-phase signals (ROEs) assigned on G20 phase-TOCSY spectrum (in red, Figure 6B). We identified inter-residue connections between units: A1  $\rightarrow$  E6 (1); E1  $\rightarrow$  A3 (2); B1  $\rightarrow$  D4 (3); D1  $\rightarrow$  E6 (4) and C1  $\rightarrow$  D3 (5) (Table II and red numbered arrows in Figure 6B). The sole glycoside bond of unit C (C [ $\alpha$ 1  $\rightarrow$  3] D) suggests that is a nonreduction terminal, and thus must be a branching. Although ROE connections between monosaccharide residues do not allow any clear proposal for a repeating unit oligosaccharide structure, Figure 7 depicts some substructures derived from NMR analyses of G20. In conclusion, despite the high complexity, insufficient sample and lack of reference data, our NMR analyses allowed us to determine some structural features of the glucan (G20) with reduced sulfate content (sulfate:hexose molar ratio  $\sim$ 0.16) and molecular size (20 kDa) present in *S. alba*.

### Sulfated polysaccharides from *S. alba* self-interact efficiently with low calcium

We performed AFM/SMFS assays to evaluate the calcium concentration needed to promote self-interactions of G20 from *S. alba*. Assessments of self-interaction forces of G20 with different calcium concentrations (1  $\rightarrow$  10 mM CaCl<sub>2</sub>) were performed by using a well-established method for immobilization of biomolecules with a hetero-bifunctional PEG linker (Figure 8A), which adds distance and steric flexibility for the binding partners and reduces unspecific interactions



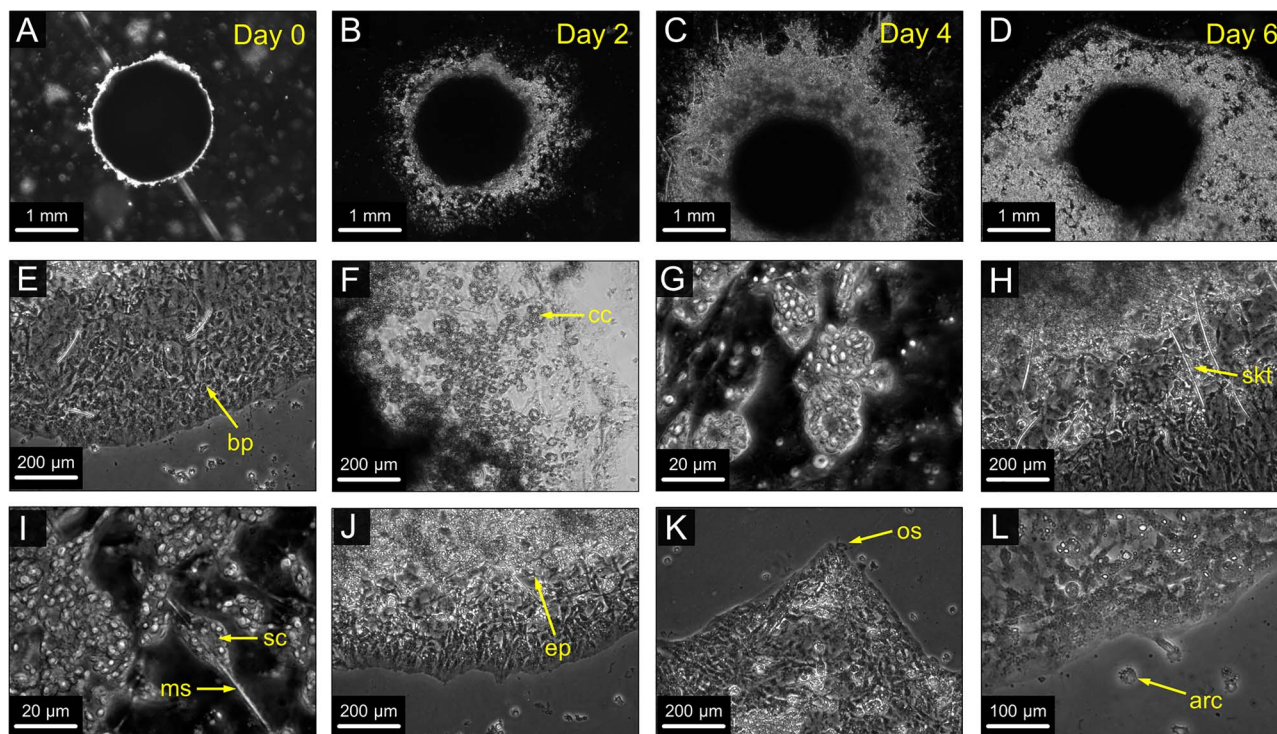


**Figure 4.** Development of new sponges from *Spongilla alba* gemmules. Gemmules incubated in natural water from Lake Carapebus hatched after 8 days (A) and passed through further development for the next 6 days until they became fully functional miniature sponges (B–D). (E) Formation of basopinacoderm (bp). (F) Choanocyte chambers (cc) component of aquiferous system. (G) Clump of archeocytes undergoing differentiation to give origin to choanocyte chambers. (H) Formation of siliceous skeleton (skt). (I) Details of spiculogenesis showing a sclerocyte (sc) secreting a megasclere (ms). (J–K) Formation of exopinacoderm (ep) and osculum (os). (L) archeocytes (arc) released by sponges in formation. This figure is available in black and white in print and in colour at *Glycobiology* online.

(Hinterdorfer et al. 1996). Homologous interactions between G20 yielded typical force curves in the presence but not in the absence of calcium (Figure 8B). Our SMFS assays revealed that G20-G20 interactions in media deprived of calcium (CMFFW-T + 5 mM EDTA) achieve binding probability and average dissociation force ( $F_{\max}$ ) significantly lower ( $P < 0.05$ ) than in media containing different concentrations of calcium (CMFFW-T + 1 → 10 mM  $\text{CaCl}_2$ ), thus confirming that G20 self-interactions are calcium-dependent (Figure 8C). G20 reached highest  $F_{\max}$  (174 pN) and binding probability (58%) when subjected to CMFFW-T supplemented with 1 mM  $\text{CaCl}_2$  (Figure 8C). Considering that AF SPs of marine sponges require 10 mM calcium to achieve maximum  $F_{\max}$  (Popescu et al. 2003), our results indicate that G20 is able to self-interact efficiently with less (ca. 10-fold lower) exogenous calcium.

## Discussion

Data on calcium concentration of rivers and lakes harboring freshwater sponges are scarce and uncertain; nevertheless, partial information available in distinct reports allowed us to trace some correlations. Nine species of freshwater sponges, including *Metania reticulata*, *Trochospongilla paulula* and *Oncosclera navicella*, were found inhabiting waters with very low calcium (~0.25 mg/L) at the River Negro (Brazil) (Küchler et al. 2000; Volkmer-Ribeiro 2012). Similarly, the freshwater sponge *Lubomirskia baikalensis*, along with other 14 species that comprise the family Lubomirskidae, which are endemic of the Lake Baikal (Russia), can also thrive in calcium-deficient (15–18 mg/L) waters (Rahmi et al. 2008; Khanaev et al. 2018). We also

find that *S. alba*'s habitat has calcium concentration notably lower (~50-fold) than seawater. Besides the examples outlined above, the reduced calcium levels (1–2 mg/L) typical of inland waters (Potaszniak and Szymczyk 2015) allow us to speculate that most species of freshwater sponges should also be adapted to colonize calcium-poor aquatic environments.

Several reports available in the literature have shown that cells of marine sponges demand approximately 400 mg/L (10 mM) calcium to undergo physiological aggregation (e.g. Misevic et al. 2004; Vilanova et al. 2009). Moreover, in vitro assays performed with microbeads coated with SPs of AFs of different marine sponges (e.g. *D. anchorata*, *C. prolifera* and *Halichondria panicea*) have already demonstrated that the SP-SP interactions responsible for sponge cell adhesion operate at physiological (10 mM) calcium concentration (e.g. Bucior et al. 2004; Vilanova et al. 2016). Our in vitro assays demonstrated that cells of the freshwater sponge *S. alba* require approximately 40-fold less calcium than cells of marine sponges to aggregate in an effective manner, which explains its capability to retain multicellular morphology in the calcium-poor (~0.2 mM) waters of the Lake Carapebus.

Modified seawater-based media have already been used to produce primmorphs from cells of different marine sponges, such as *Suberites domuncula*, *Hymeniacidon heliophila* and *Dysidea avara*; however, all of those media contained standard (10 mM) calcium concentrations (Müller et al. 2000; Natalio et al. 2010; Vilanova et al. 2010). Despite the lack of direct evidence, formation of primmorphs from cells of marine sponges with substantially lower calcium concentrations is unlikely considering that they have been shown to require 10 mM calcium to aggregate (e.g. Misevic et al. 2004;

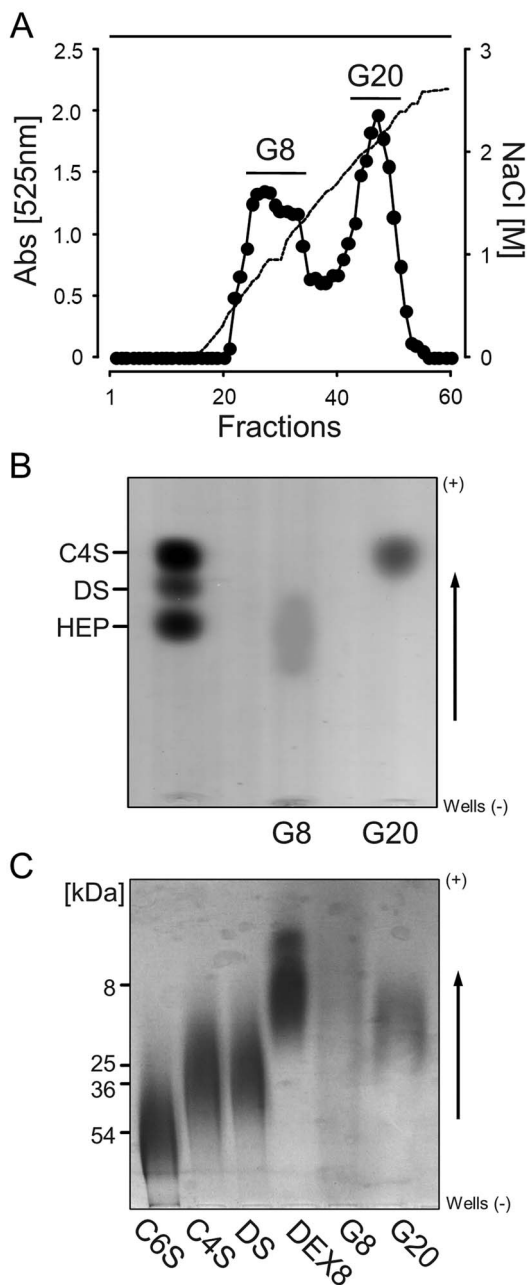


**Figure 5.** Purification of sulfated polysaccharides from *Spongilla alba*. (A) Crude polysaccharide extracts from *S. alba* applied into a Q-Sepharose column and then eluted through a linear gradient of 0 → 3 M NaCl (black pointed line) monitored by metachromasy ( $Abs_{525nm}$ ) yielded two fractions (G8 and G20). (B) Agarose gel electrophoresis of GAG standards (HEP, DS and C4S), G8 and G20. (C) Polyacrylamide gel electrophoresis of G8, G20 and the standards C6S (~54 kDa), C4S (~36 kDa), DS (~25 kDa) and DEX8 (~8 kDa). This figure is available in black and white in print and in colour at *Glycobiology* online.

Bucior et al. 2004; Vilanova et al. 2009). A recent study on spiculation of the freshwater sponge *L. baikalensis* was performed with primmorphs kept in culture for up to 9 months in media prepared using Lake Baikal water, thus containing reduced calcium concentration (~0.4 mM) (Annenkov and Danilovtseva 2016). Primmorphs from *S. alba* cells produced with low calcium (~0.2 mM) presented

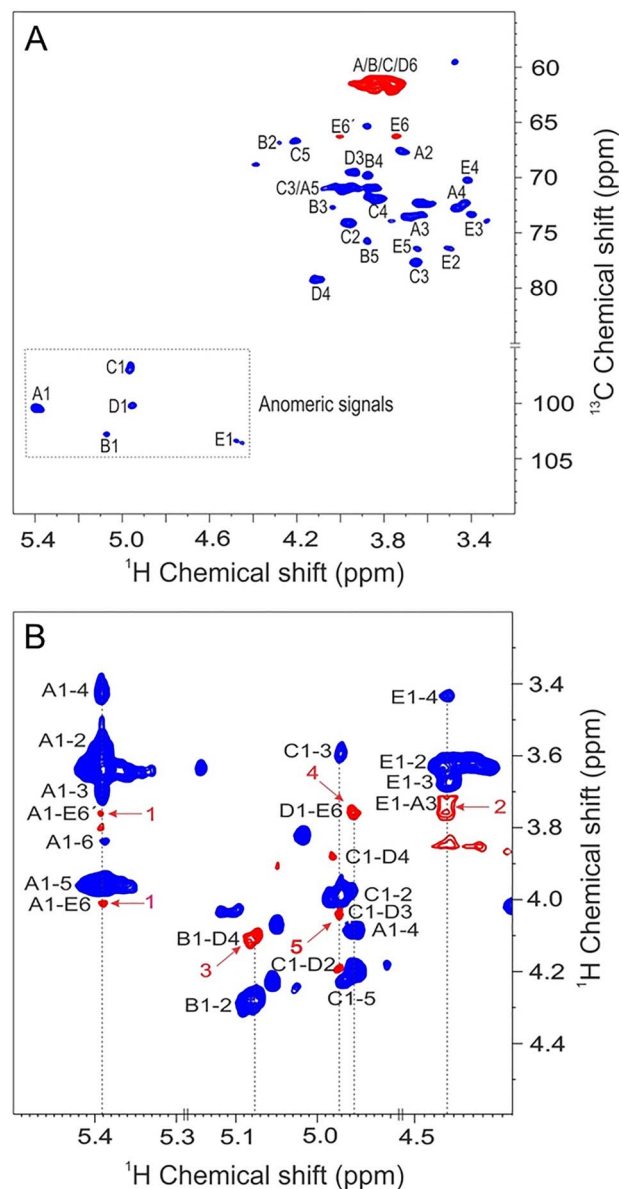


**Figure 6.** NMR spectra of G20. (A)  $^1H/^{13}C$  HSQC spectrum; in-phase signals (in blue) correspond to CH or  $CH_3$  and signals in anti-phase (in red) to  $CH_2$  groups. (B)  $^1H/^1H$  phase-TOCSY spectrum; signals of spin systems of each unit (vertical lines) are in-phase (in blue) and signals of neighboring residues (red numbered arrows) are in anti-phase (in red, ROEs).  $^1H$  and  $^{13}C$  chemical shifts and quantifications of the units (A → E) annotated on the spectra are available in Table I. This figure is available in black and white in print and in colour at *Glycobiology* online.

formation dynamics, morphological traits and cell composition alike to those produced by cells of the marine sponge *H. heliophila* with 10 mM calcium (Vilanova et al. 2010), which suggests that despite contrasting calcium requirements, primmorphs from freshwater and marine sponges are generated in a similar manner.

A study published in 1978 showed that calcium is essential for hatching of gemmules of the freshwater sponge *Spongilla lacustris* and that it is able to overcome inhibitory effects of some divalent cations ( $Zn^{2+}$ ,  $Mn^{2+}$ ,  $Ba^{2+}$  and  $Sr^{2+}$ ) during hatching and initial development (Ostrom and Simpson 1978). Information available in this early study along with the results presented here is the only report

**Table I.**  $^1\text{H}$  and  $^{13}\text{C}$  chemical shifts of G20 units

Unit	Proportion (%) <sup>a</sup>	Chemical shift (ppm)					
		H1/C1	H2/C2	H3/C3	H4/C4	H5/C5	H6/C6
A	~30	5.39/102.7	3.72/69.8	3.70/75.7a	3.46/74.8	4.01/71.0	3.84/64.5
B	~10	5.08/102.9	<b>4.29/66.8</b>	4.03/79.8	3.91/72.3	3.88/75.5	3.76/63.3
C	~20	4.98/96.7	3.97/76.4	3.66/72.9	3.88/73.9	4.21/68.7	3.92/63.7
D	~20	4.96/100.1	<b>4.21/68.7</b>	4.04/73.3	<b>4.10/81.5</b>	3.95/74	3.85/64.0
E	~20	4.50/103.5	3.50/74.6	3.58/72.4	3.43/72.5	3.65/78.6	4.01; 3.75/68.5

<sup>a</sup>Proportions of the units were calculated by integrating their H1/C1 signals on the HSQC spectrum (Mourão et al. 2018). Sulfation and glycosylation sites in bold and italics, respectively.

**Table II.** Connection points between G20 units determined with the  $^1\text{H}/^1\text{H}$  phase-TOCSY spectrum

Connection <sup>a</sup>	Chemical structure	Chemical shift ( $^1\text{H}/^1\text{H}$ ppm)
A1 → E6 (1)	$\alpha$ -Glc [1 → 6] $\beta$ -Glc	5.39/4.01 5.39/3.75
E1 → A3 (2)	$\beta$ -Glc [1 → 3] $\alpha$ -Glc	4.50/3.70
B1 → D4 (3)	$\alpha$ -Glc2S [1 → 4] $\alpha$ -Glc2S	5.08/4.10
D1 → E6 (4)	$\alpha$ -Glc2S [1 → 6] $\beta$ -Glc	4.96/4.01
C1 → D3 (5)	$\alpha$ -Glc2S [1 → 4] $\alpha$ -Glc	4.98/4.03

<sup>a</sup>See ROE signal cross-peaks (numbered red arrows) on the phase-TOCSY spectrum (Figure 6B).

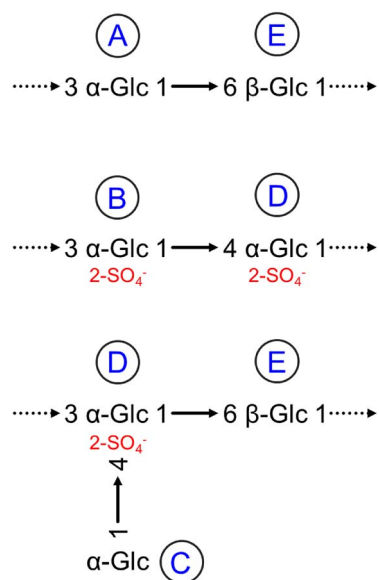


**Figure 7.** Structural features of G20. Units (A → E) ascribed on NMR spectra are indicated in blue and sulfation sites in red. This figure is available in black and white in print and in colour at *Glycobiology* online.

to date on the role of calcium in the development of new sponges from gemmules. Although we have failed in hatching gemmules of *S. alba* by using M-medium, previous studies have proven that it is possible to hatch gemmules of different species with this artificial medium (e.g. Schill et al. 2006; Bart et al. 2019). In addition to minor differences in the concentration of some constituents, our modified medium does not contain magnesium, which is present in standard M-media (Rasmont 1961). Considering that LCW deprived only of calcium

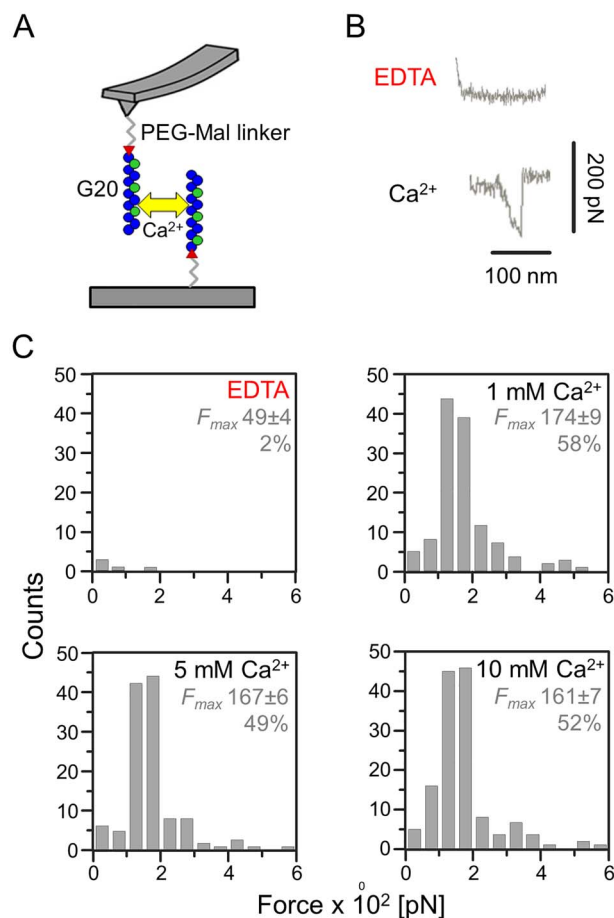


**Figure 8.** Single molecule force spectroscopy analyses of the sulfated polysaccharide from *Spongilla alba*. (A) Schematic view of the expected topography of calcium-mediated interactions between G20 polysaccharides from *S. alba* (double arrow, in yellow) immobilized onto atomic force microscopy cantilevers and substrates with a heterobifunctional PEG-Mal linker. (B) Typical self-binding force curves of G20 acquired in the presence (1 mM  $\text{CaCl}_2$ ) or absence (5 mM EDTA) of calcium with constant approach and retract velocities (2000 nm/s). (C) Force histograms of self-interactions of G20 in the absence (EDTA) or presence (1, 5 and 10 mM  $\text{CaCl}_2$ ) of calcium used to calculate average dissociation forces ( $F_{\text{max}}$ , in pN, mean  $\pm$  S.E.) and binding probabilities (% of assays yielding valid force curves). This figure is available in black and white in print and in colour at *Glycobiology* online.

(supplemented with EGTA) has also failed and that there is no evidence on its physiological relevance for siliceous sponges, the unsuccessful hatching with our M-medium should not be due to the lack of



magnesium. The dark water of Lake Carapebus is loaded of dissolved organic carbon and other elements such as phosphates and nitrates (Marotta et al. 2010), which could be required to trigger hatching, thus allowing us to conclude that gemmules of *S. alba* require a complex set of micronutrients to hatch and produce new sponges.

Despite requiring specific media to hatch, the development of new sponges from gemmules of *S. alba* is similar to those described for other freshwater sponges, such as *E. fluviatilis* and *S. lacustris* (Schill et al. 2006; Bart et al. 2019). Assays with gemmules have already been used in molecular and physiological investigations. A study based on *Ephydatia muelleri* gemmules demonstrated that the homeobox gene *EmH-3* is overexpressed in totipotent archeocytes but not in somatic cells (Richelle-Maurer and Van de Vyver 1999). Assessments of microRNAs expression showed that cells of quiescent gemmules of *S. lacustris* contain increased amounts of the stress protein Hsp-70 (Schill et al. 2006). In addition to molecular studies, gemmules from *E. fluviatilis* were also used in spiculogenesis and innate immunity investigations (Funayama et al. 2005; Bart et al. 2019). These findings showed that hatching of gemmules is a valuable model for studying the developmental biology of sponges and to trace molecular correlations between these ancestral animals and other metazoans.

Marine sponges SPs are among the most complex found in nature, which makes structural characterization a difficult task, even by employing high-resolution NMR techniques (Vilanova et al. 2008, 2016). Despite high complexity and scarce sample available to acquire spectra, our NMR analyses indicated that the glucan G20 purified from *S. alba* is composed of a central backbone of non- and 2-sulfated  $\alpha$ - and  $\beta$ -glucose units decorated with branches of  $\alpha$ -glucose. Moreover, we demonstrate that G20 is less sulfated and has a molecular size significantly smaller than marine sponges SPs; for example, SPs from *D. anchorata* and *C. prolifera* have molecular masses (~200 kDa) ca. 10-fold higher than G20 (Vilanova et al. 2008, 2016; Garcia-Manyes et al. 2006). Although AFs had been detected in the freshwater sponge *E. fluviatilis* almost 50 years ago (Fernández-Busquets and Burger 1999), the chemical structure of their constituents have never been analyzed in detail and, therefore, it is the first report of the composition of a freshwater sponge SP.

Although Expressed Sequence Tag (EST) surveys have already found genes related to cell-adhesion receptors, extracellular matrix/basement membrane and cytoskeletal-linker proteins in the homoscleromorph sponge *Oscarella carmella*, there is no direct evidence on their participation in cell–cell adhesion and recognition in sponges to date (Nichols et al. 2006). On the other hand, sponge cell aggregation assays in the presence of antibodies against AF SP-epitopes, as well as a variety of cell-free assessments, including micro-beads aggregation, membrane blot, affinity chromatography and SMFS assays, have shown that cell adhesion in marine sponges is sustained by carbohydrate–carbohydrate interactions promoted by SP components of AFs Fernández-Busquets et al. 2009; Vilanova et al. 2016). According to the “cooperative binding model” proposed by Fernández-Busquets et al. (2009), the firmness and stability of cell–cell adhesion mediated by AFs rely on multivalent calcium-mediated self-interactions between their SPs. Our AFM/SMFS assays show that the self-interactions between G20 responsible for sustaining cell adhesion of the freshwater sponge *S. alba* are also calcium-dependent.

Previous reports based on AFM/DFS analyses demonstrated that both intact AFs and purified SPs from *C. prolifera* achieve self-interaction forces far higher in calcium-rich (10 mM) than in calcium-deficient (2 mM) assays (Popescu et al. 2003). Self-interactions of SPs isolated from AFs of different marine sponges have shown to reach

self-interaction forces between 180 and 310 pN with physiological (10 mM) calcium concentration (Bucior et al. 2004). Our AFM/SMFS assays revealed that G20 from *S. alba* achieves dissociation force (174 pN) equivalent to those of SPs from marine sponges with 10-fold less calcium (1 mM). We hypothesized that such an ability of G20 to self-interact efficiently with less calcium could be related to smaller repulsive effects between sulfate groups in the presence of media with lower NaCl concentration (Vilanova et al. 2016).

Although paleobiogeography of freshwater sponges is relatively well documented (e.g. Pronzato et al. 2017), studies correlating distribution of modern species and water chemistry are scarce and fragmented. We demonstrate here that *S. alba* is able to retain multicellular morphology with 0.2 mM but not 0.1 mM calcium while other species can survive in water bodies with far lower (<0.01 mM) calcium concentrations (Küchler et al. 2000; Volkmer-Ribeiro 2012), which indicates that freshwater sponges have distinct and specific calcium requirements, and thus, it must be an environmental factor intrinsically related to their biogeographical distributions. We also find that freshwater sponges are able to sustain cell-adhesion promoted by AFs with calcium concentrations far lower than that required by marine sponges (Fernández-Busquets et al. 2009; Vilanova et al. 2016). Such a capability of freshwater sponges to thrive in aquatic environments with low calcium must have been a crucial evolutionary adaptation for colonizing inland waters.

## Material and methods

### Sponge samples and water analyses

The freshwater sponge *S. alba* (Supplementary Figure S1) was collected by SCUBA dive at Lake Carapebus, Rio de Janeiro State, SE Brazil (Supplementary Figure S1). Sponge samples for in vitro assays were transported to the laboratory immersed in lake's water and kept in an aquarium at 18°C until processing and samples for extraction of SPs were fixed in 70% ethanol immediately after collection. Analysis of the chemical composition of Lake Carapebus water was performed by the contract research organization (CRO) Eurofins-Innolab (Rio de Janeiro, Brazil). Water samples were collected by following the CRO instructions and the chemical parameters quantified with standard tests (see: <https://www.astm.org/Standards/water-testing-standards.html>, St. Louis, United States). All reagents and standards were from Sigma-Aldrich unless otherwise stated.

### Cell aggregation assays

Cells from *S. alba* were chemically dissociated as follows: sponge tissues were cut into small pieces (2–3 mm<sup>3</sup>) and incubated in calcium- and magnesium-free artificial freshwater (CMFFW) composed of 2 mM NaCl, 0.2 mM Na<sub>2</sub>SO<sub>4</sub>, 0.1 mM KCl and 10 mM HEPES (pH 8.0), supplemented with 2.5 mM EDTA (CMFFW+E), for 1 h at room temperature, and then filtered (40  $\mu$ m mesh), harvested by centrifugation (80g, 10 min), resuspended in CMFFW and stored at 4°C until further utilization. Aggregation assays were performed in triplicate by incubating 10<sup>9</sup> cells in 5 mL CMFFW supplemented with different concentrations of CaCl<sub>2</sub> (0.1  $\rightarrow$  0.5 mM) or CMFFW+E for 1 h at room temperature. The number and size of cell aggregates (10 random fields per plate) formed at different calcium concentrations were quantified using a Leica DC 300 microscope (Leica; Weitzlar, Germany) and compared by analysis of variance (ANOVA) with Tukey post hoc test by using the software Origin 8.0 (Origin Lab).

### Primmorph formation

Primmorphs were formed (in triplicate) from approximately  $10^9$  cells of *S. alba*, which were kept in culture for 5 days in 5 mL CMFFW supplemented with 0.25 or 0.5 mM  $\text{CaCl}_2$  and tylosin+kanamycin antibiotics (0.01 mg/mL of each) at 18°C, by following procedures previously described for marine sponges (Custódio et al. 1998). Cultures were monitored with a Leica DC 300 microscope. Mature primmorphs formed at 0.25 mM  $\text{CaCl}_2$  were fixed in 10% glutaraldehyde for 24 h at 4°C, sectioned on a microtome (10  $\mu\text{m}$ ) and stained with 4% toluidine blue for histological examinations using a Axio Imager A1 microscope (Zeiss, Oberkochen, Germany). Three primmorphs formed at 0.25 mM  $\text{CaCl}_2$  were dissociated with CMFFW+E and then their cells were fixed in 10% glutaraldehyde for 24 h at 4°C, quantified with an Axio Imager A1 microscope (10 fields per primmorph) and compared by ANOVA.

### Gemmule hatching

Gemmules (five per plate, in triplicate) from *S. alba* (five specimens) were sterilized with 1%  $\text{H}_2\text{O}_2$  in modified M-medium (0.2 mM  $\text{Na}_2\text{SO}_4$ , 0.5 mM  $\text{NaHCO}_3$ , 0.5 mM KCl and 0.25 mM  $\text{Na}_2\text{SiO}_3$ ; pH 8.0) (Rasmont 1961) supplemented with 0.5 mM  $\text{CaCl}_2$  for 5 min at 4°C, kept for 48 h in M-medium +0.5 mM  $\text{CaCl}_2$  or filtered (0.22  $\mu\text{m}$  mesh) Lake Carapebus water (LCW) and then incubated at 18°C in sterile conditions in 5 mL of either (i) M-medium supplemented with different concentrations of  $\text{CaCl}_2$  (0.1  $\rightarrow$  0.5 mM) or with 2.5 mM EDTA, (ii) LCW, (iii) LCW supplemented with 2.5 mM EDTA or (iv) LCW supplemented with 2.5 mM EGTA. After hatching, initial development of the sponges was followed with a Leica DC 300 microscope.

### Extraction and purification of sulfated polysaccharides

Tissues of *S. alba* were cut into small pieces, immersed in acetone (three times) and dried at 60°C. SPs were extracted from the dried tissues (~50 g) through proteolytic digestion with papain and then partially purified with cetylpyridinium and ethanol precipitations (Stelling et al. 2019). Crude polysaccharide extracts (~5 mg) were applied into a Q-Sepharose XL column (GE healthcare; Illinois, United States), linked to a HPLC system (Shimadzu; Tokyo, Japan), equilibrated with 20 mM Tris-HCl and 1 mM EDTA (pH 7.4) and then eluted through a linear gradient of 0  $\rightarrow$  3 M NaCl. Fractions of 0.5 mL were collected, checked for metachromasy with 1,9-dimethylmethylene blue and then pooled as two distinct fractions named G8 and G20, dialyzed against distilled water, lyophilized and stored at -20°C for further utilization (Stelling et al. 2019).

### Agarose gel electrophoresis

*S. alba* SPs isolated with anion-exchange chromatography were analyzed by agarose gel electrophoresis (Stelling et al. 2019). G8, G20 and the glycosaminoglycan (GAG) standards heparin (HEP), dermatan sulfate (DS) and chondroitin 4-sulfate (C4S) were applied (5  $\mu\text{g}$  of each) into a 0.5% agarose gel in 0.05 M 1,3-diaminopropane acetate (pH 9.0). Electrophoresis was performed at 100 V for approximately 1 h and then the gel was fixed with 0.1% *N*-cetyl-*N,N,N*-trimethylammonium bromide for 12 h at room temperature, dried and stained with 0.1% toluidine blue in 0.1:5:5 (v/v) acetic acid:ethanol:water.

### Polyacrylamide gel electrophoresis

The molecular sizes of *S. alba* SPs were estimated by polyacrylamide gel electrophoresis (Stelling et al. 2019). Fractions G8 and G20 and

the standards dextran sulfate ( $M_r \sim 8000$ ; DEX8), chondroitin 6-sulfate (C6S), C4S and DS (10  $\mu\text{g}$  of each) were applied into a 1-mm-thick 7.5% polyacrylamide gel in 60 mM Tris-HCl (pH 8.6). Electrophoresis was performed at 100 V for approximately 40 min at room temperature, and then the gel was stained with 0.1% toluidine blue in 1% acetic acid.

### Chemical analyses

Chemical analyses were performed as described elsewhere (Vilanova et al. 2009; Stelling et al. 2019). Briefly, the total hexose content of *S. alba* SPs was estimated by phenol- $\text{H}_2\text{SO}_4$  reaction and the presence of hexuronic acid or pyruvated sugars with carbazole reaction. After acid hydrolysis with 6.0 M trifluoroacetic acid for 5 h at 100°C, G8 and G20 had their relative sulfate contents estimated by the  $\text{BaCl}_2$ -gelatin method. Monosaccharide compositions were determined via GC/MS (Shimadzu) by analyzing alditol acetate derivatives produced by G20.

### NMR analyses

NMR spectra of G20 were recorded using a DRX 800 MHz spectrometer (Bruker; Billerica, United States) with triple-resonance probe as previously described (Vilanova et al. 2016). About 2 mg of G20 was dissolved in 0.5 mL 99.9% deuterium oxide (Cambridge Isotope Laboratory; Cambridge, United States), and then the spectra were recorded at 50°C with HOD (deuterium oxide) suppression by presaturation. 1D  $^1\text{H}$  NMR spectrum was recorded with 16 scans. Phase-sensitive  $^1\text{H}/^1\text{H}$  MLEV17 TOCSY spectrum (4046  $\times$  400 points) was acquired with spin-lock field of 10 kHz and mix time of 80 ms.  $^{13}\text{C}/^1\text{H}$  multiplicity-edited HSQC spectrum (1024  $\times$  256 points) was acquired with globally optimized alternating phase rectangular pulses for decoupling (GARP).  $^1\text{H}$  and  $^{13}\text{C}$  chemical shifts were calibrated (0 ppm) with basis on signals from external standards trimethylsilyl propionic acid and methanol, respectively. Spectra were processed using the software Top-Spin 3.5 (Bruker).

### Single-molecule force spectroscopy assays

Self-binding forces of G20 from *S. alba* at different concentrations of calcium were measured with a MFP-3D atomic force microscope (Asylum Research; Abingdon, United Kingdom). G20 was immobilized on gas-phase amino-silanized mica substrates and silicon nitride tip (NP-S) cantilevers (Bruker) by using a *N*-hydroxysuccinimide-poly-(ethylene glycol)-maleimide (NHS-PEG-MAL) linker of 4750 Da (Iris Biotech GmbH; Marktredwitz, Germany), as described elsewhere (Vilanova et al. 2016). SMFS assays were performed at room temperature by approaching and separating cantilevers and substrates functionalized with G20 in CMFFW-T (2 mM NaCl, 0.2 mM  $\text{Na}_2\text{SO}_4$ , 0.1 mM KCl and 20 mM Tris, pH 8.0) supplemented with 5 mM EDTA or different concentrations of  $\text{CaCl}_2$  (1  $\rightarrow$  10 mM). Spring constants of the cantilevers were determined by the thermal noise method (Lévy and Maaloum 2002). Approximately 2000 force curves were recorded with constant approach and retract velocities (2000 nm/s) and afterwards analyzed with custom-made MATLAB-based software (Math Works; Natick, United States) in order to calculate molecular adhesion forces and elasticity. Force histograms were fitted as normal curves to obtain the average dissociation forces ( $F_{max}$ ) by using the software Origin 8.0 (Origin Lab).

## Supplementary data

Supplementary data for this article is available online at <http://glycob.oxfordjournals.org/>.

## Conflicts of interest statement

The authors declare that they have no conflict of interest.

## Abbreviations

AF, sponge aggregation factor ; AFM, atomic force microscopy ; CMFFW, calcium- and magnesium-free artificial freshwater ; DFS, dynamic force spectroscopy ; EST, expressed sequence tag ;  $F_{max}$ , average dissociation force ; G8 and G20, sulfated polysaccharides from *S. alba* ; HSQC, heteronuclear single quantum coherence ; LCW, Lake Carapebus Water ; pN, piconewton ; ppt, mg/ton ; SMFS, single molecule force spectroscopy ; SP, sulfated polysaccharide ; TOCSY, total correlation spectroscopy.

## Acknowledgements

We thank Carapebus municipal government (Rio de Janeiro State, Brazil) and Bianca Glauser for supporting collection of biological and water samples and Adriana Piquet and Mirian Funes for technical assistance. ISGlobal and IBEC are members of the CERCA (Centres de Recerca de Catalunya). This research is part of ISGlobal's Program on Molecular Mechanisms of Malaria, which is partially supported by the Fundación Ramón Areces.

## Funding

This work was supported by several Brazilian grants from Fundação de Amparo à Pesquisa do Estado do Rio de Janeiro (FAPERJ); Conselho Nacional de Desenvolvimento Científico e Tecnológico (CNPq) and Coordenação de Aperfeiçoamento do Pessoal de Nível Superior (CAPES); Spanish grants from Fundación Carolina (CAPES002/2011), Ministerio de Economía y Competitividad (BIO2011-25039 and BIO2014-52872-R), Generalitat de Catalunya (2014-SGR-938) and Program “Centro de Excelencia Severo Ochoa 2019-2023” (CEX2018-000806-S) and German grants from the German Science Foundation (DFG) (AN 370/6-2 and AN 370/8-1) as well from Bielefeld University Medical Research Fund (LUMA).

## References

Abedin M, King N. 2010. Diverse evolutionary paths to cell adhesion. *Trends Cell Biol.* 20:734–742.

Annenkov VV, Danilovtseva EN. 2016. Spiculogenesis in the siliceous sponge *Lubomirskia baicalensis* studied with fluorescent staining. *J Struct Biol.* 194:29–37.

Bart MC, de Vet SJ, de Bakker DM, Alexander BE, van Oevelen D, van Loon EE, van Loon JJWA, de Goeij JM. 2019. Spiculous skeleton formation in the freshwater sponge *Ephydatia fluviatilis* under hypergravity conditions. *PeerJ.* 6:e6055.

Blumbach B, Pancer Z, Diehl-Seifert B, Steffen R, Münkner J, Müller I, Müller WE. 1998. The putative sponge aggregation receptor: Isolation and characterization of a molecule composed of scavenger receptor cysteine-rich domains and short consensus repeats. *J Cell Sci.* 111: 2635–2644.

Bucior I, Scheuring S, Engel A, Burger MM. 2004. Carbohydrate-carbohydrate interaction provides adhesion force and specificity for cellular recognition. *J Cell Biol.* 165:529–537.

Custódio MR, Prokic I, Steffen R, Koziol C, Borojevic R, Brummer F, Nickel M, Muller WE. 1998. Primmorphs generated from dissociated cells of the sponge *Suberites domuncula*: A model system for studies of cell proliferation and cell death. *Mech Ageing Dev.* 105:45–59.

Erpenbeck D, Weier T, de Voogd NJ, Wörheide G, Sutcliffe P, Todd JA, Michel E. 2011. Insights into the evolution of freshwater sponges (Porifera: Demospongiae: Spongillina): Barcoding and phylogenetic data from Lake Tanganyika endemics indicate multiple invasions and unsettle existing taxonomy. *Mol Phylogenet Evol.* 61:231–236.

Fernández-Busquets X. 2010. Cambrian explosion. In: Kehler-Sawatzki H, editor. *Encyclopedia of life sciences*. Chichester: John Wiley & Sons. p. 1–10.

Fernández-Busquets X, Burger MM. 1999. Cell adhesion and histocompatibility in sponges. *Microsc Res Tech.* 44:204–218.

Fernández-Busquets X, Burger MM. 2003. Circular proteoglycans from sponges: First members of the spongican family. *Cell Mol Life Sci.* 60:88–112.

Fernández-Busquets X, Körnig A, Bucior I, Burger MM, Anselmetti D. 2009. Self-recognition and  $Ca^{2+}$  dependent carbohydrate-carbohydrate cell adhesion provide clues to the Cambrian explosion. *Mol Biol Evol.* 26:2551–2561.

Funayama N. 2013. The stem cell system in demosponges: Suggested involvement of two types of cells: Archeocytes (active stem cells) and choanocytes (food-entrapping flagellated cells). *Dev Genes Evol.* 223:23–38.

Funayama N, Nakatsukasa M, Kuraku S, Takechi K, Dohi M, Iwabe N, Miyata T, Agata K. 2005. Isolation of Ef silicatein and Ef lectin as molecular markers for sclerocytes and cells involved in innate immunity in the freshwater sponge *Ephydatia fluviatilis*. *Zool Sci.* 22:1113–1122.

García-Manyes S, Bucior I, Ros R, Anselmetti D, Sanz F, Burger MM, Fernández-Busquets X. 2006. Proteoglycan mechanics studied by single-molecule force spectroscopy of allotypic cell adhesion glycans. *J Biol Chem.* 281:5992–5999.

Hinterdorfer P, Baumgartner W, Gruber HJ, Schilcher K, Schindler H. 1996. Detection and localization of individual antibody-antigen recognition events by atomic force microscopy. *Proc Natl Acad Sci USA.* 93:3477–3481.

Jarchow J, Fritz J, Anselmetti D, Calabro A, Hascall VC, Gerosa D, Burger MM, Fernández-Busquets X. 2000. Supramolecular structure of a new family of circular proteoglycans mediating cell adhesion in sponges. *J Struct Biol.* 132:95–105.

Johnston IS, Hildemann WH. 1982. Cellular defense systems of the Porifera. In: Cohen N, Sigel MM, editors. *Phylogeny and ontogeny*. Boston: Springer. p. 37–57.

Khanaev IV, Kravtsova LS, Maikova OO, Bukshuk NA, Sakirko MV, Kulakova NV, Butina TV, Nebesnykh IA, Belikov SI. 2018. Current state of the sponge fauna (Porifera: Lubomirskiidae) of Lake Baikal: Sponge disease and the problem of conservation of diversity. *J Great Lakes Res.* 44:77–85.

Küchler IL, Miekeley N, Forsberg BR. 2000. A contribution to the chemical characterization of rivers in the Rio Negro Basin, Brazil. *J Braz Chem Soc.* 11:286–292.

Lévy R, Maaloum M. 2002. Measuring the spring constant of atomic force microscope cantilevers: Thermal fluctuations and other methods. *Nanotechnology.* 13:33–37.

Maloff AC, Rose C, Beach R, Samuels BM, Calmet CC, Erwin DH, Poirier GH, Yao M, Simons RJ. 2010. Possible animal body fossils in pre-Marinoan limestones from South Australia. *Nat Geosci.* 3:653–659.

Manconi R, Pronzato R. 2008. Gemmules as a key structure for the adaptive radiation of freshwater sponges: A morphofunctional and biogeographical study. In: Custódio MR, et al., editors. *Porifera research: Biodiversity, innovation, and sustainability*. Rio de Janeiro: Museu Nacional. p. 61–77.

Manconi R, Pronzato R. 2016. How to survive and persist in temporary freshwater? Adaptive traits of sponges (Porifera: Spongillida): A review. *Hydrobiologia.* 782:11–22.



- Marotta H, Duarte CN, Pinho L, Enrich-Prast A. 2010. Rainfall leads to increased pCO<sub>2</sub> in Brazilian coastal lakes. *Biogeosciences*. 7:1607–1614.
- Millero FJ, Feistel R, Wright DG, McDougall TJ. 2008. The composition of standard seawater and the definition of the reference-composition salinity scale. *Deep Sea Res Part I Oceanogr Res Pap.* 55:50–72.
- Misevic GN, Guerardel Y, Sumanovski LT, Slomianny MC, Demarty M, Ripoll C, Karamanos Y, Maes E, Popescu O, Strecker G. 2004. Molecular recognition between glycoconectins as an adhesion self-assembly pathway to multicellularity. *J Biol Chem.* 279:15579–15590.
- Mourão PA, Vilanova E, Soares PA. 2018. Unveiling the structure of sulfated fucose-rich polysaccharides via nuclear magnetic resonance spectroscopy. *Curr Opin Struct Biol.* 50:33–41.
- Müller WE, Böhm M, Batel R, De Rosa S, Tommonaro G, Müller IM, Schröder HC. 2000. Application of cell culture for the production of bioactive compounds from sponges: Synthesis of avarol by primmorphs from *Dysidea avara*. *Nat Prod.* 63:1077–1781.
- Natalio F, Mugnaioli E, Wiens M, Wang X, Schröder HC, Tahir MN, Tremel W, Kolb U, Müller WE. 2010. Silicatein-mediated incorporation of titanium into spicules from the demosponge *Suberites domuncula*. *Cell Tissue Res.* 339:429–436.
- Nichols SA, Dirks W, Pearse JS, King N. 2006. Early evolution of animal cell signaling and adhesion genes. *Proc Natl Acad Sci USA.* 103:12451–12456.
- Ostrom KK, Simpson LT. 1978. Calcium and the release from dormancy of freshwater sponge Gemmules. *Dev Biol.* 64:332–338.
- Popescu O, Checiu I, Gherghel P, Simon Z, Misevic GN. 2003. Quantitative and qualitative approach of glycan-glycan interactions in marine sponges. *Biochimie.* 85:181–188.
- Potasznik A, Szymczyk S. 2015. Magnesium and calcium concentrations in the surface water and bottom deposits of a river-lake system. *J Elem.* 20:677–692.
- Pronzato R, Pisera A, Manconi R. 2017. Fossil freshwater sponges: Taxonomy, geographic distribution, and critical review. *Acta Palaeontol Pol.* 62:467–495.
- Rahmi D, Zhu Y, Umemura T, Haraguchi H, Itoh A, Chiba K. 2008. Determination of 56 elements in Lake Baikal water by high-resolution ICP-MS with the aid of a tandem preconcentration method. *Anal Sci.* 24:1513–1517.
- Rasmont R. 1961. Une technique de culture des éponges d'eau douce en milieu contrôlé. *Annales de la Société royale zoologique de Belgique.* 91:147–155.
- Richelle-Maurer E, Van de Vyver G. 1999. Temporal and spatial expression of EmH-3, a homeobox-containing gene isolated from the freshwater sponge *Ephydatia muelleri*. *Mech Ageing Dev.* 109:203–219.
- Schill RO, Pfannkuchen M, Fritz G, Köhler HR, Brümmer F. 2006. Quiescent gemmules of the freshwater sponge, *Spongilla lacustris* (Linnaeus, 1759), contain remarkably high levels of Hsp70 stress protein and hsp70 stress gene mRNA. *J Exp Zool A Comp Exp Biol.* 305:449–457.
- Stelling MP, de Bento AA, Caloba P, Vilanova E, Pavão MSG. 2019. Methods for isolation and characterization of sulfated glycosaminoglycans from marine invertebrates. *Methods Mol Biol.* 1952:55–70.
- Tovar AM, Santos GR, Capillé NV, Piquet AA, Glauser BF, Pereira MS, Vilanova E, Mourão PA. 2016. Structural and haemostatic features of pharmaceutical heparins from different animal sources: Challenges to define thresholds separating distinct drugs. *Sci Rep.* 6:35619.
- Vilanova E, Coutinho C, Maia G, Mourão PAS. 2010. Sulfated polysaccharides from marine sponges: Conspicuous distribution among different cell types and involvement on formation of in vitro cell aggregates. *Cell Tissue Res.* 340:523–531.
- Vilanova E, Coutinho CC, Mourão PAS. 2009. Sulfated polysaccharides from marine sponges (Porifera): An ancestor cell-cell adhesion event based on the carbohydrate-carbohydrate interaction. *Glycobiology.* 19:860–867.
- Vilanova E, Santos GR, Aquino RS, Valle-Delgado JJ, Anselmetti D, Fernández-Busquets X, Mourão PAS. 2016. Carbohydrate-carbohydrate interactions mediated by sulfate esters and calcium provide the cell adhesion required for the emergence of early metazoans. *J Biol Chem.* 291: 9425–9437.
- Vilanova E, Zilberberg C, Kochem M, Custódio MR, Mourão PAS. 2008. A novel biochemical method to distinguish cryptic species of genus *Chondrilla* (Demospongiae: Chondrosida) based on its sulfated polysaccharides. In: Custódio MR, et al., editors. *Porifera research: Biodiversity, innovation, and sustainability*. Rio de Janeiro: Museu Nacional. p. 653–659.
- Volkmer-Ribeiro C. 2012. Composition, distribution and substrates of the sponge fauna (Porifera: Demospongiae) at the National Park of Anavilhanas. *Neotrop Biol Conserv.* 7:188–198.